Impact of roadside conifers vegetation growth on air pollution mitigation

Article *in* Landscape and Urban Planning · January 2023

DOI: 10.1016/j.landurbplan.2022.104594

6 authors, including:


Khaled Hashad
Cornell University


Bo Yang
3M


John Gallagher
Trinity College Dublin


Richard William Baldauf
United States Environmental Protection Agency

Impact of roadside conifers vegetation growth on air pollution mitigation

Khaled Hashad[a], Bo Yang[a], John Gallagher[b], Richard Baldauf [c,d], Parikshit Deshmukh [e], K. Max Zhang[a,1]

[a] *Sibley School of Mechanical and Aerospace Engineering, Cornell University, Ithaca, NY 14853, USA*
[b] *Department of Civil, Structural & Environmental Engineering, Trinity College Dublin, the University of Dublin, Ireland*
[c] *Office of Research and Development, U.S. Environmental Protection Agency, Durham, NC, USA*
[d] *Office of Transportation and Air Quality, U.S. Environmental Protection Agency, Ann Arbor, MI, USA*
[e] *Eastern Research Group Inc., Durham, NC, USA*

Abstract

As a Nature-Based Solution, roadside green infrastructure (also known as roadside barriers) can potentially mitigate traffic-related air pollution by increasing dispersion and promoting pollutant deposition. For new and existing roadside barriers, the vegetation's physical and ecological attributes (dimensions and density) are dynamic in nature, and thus affect the barriers' pollution reduction capabilities. In this study, we first synthesized the results from existing field measurements characterizing the properties of coniferous vegetation, which show that its growth was characterized by an increase in height and a decrease in density. Motivated by this finding, a total of 75 simulations was conducted using a coupled aerodynamics and deposition model to investigate how the growth patterns of roadside vegetation barriers (e.g., heights from 2-10 m, and leaf area index (LAI) from 4-11) affects air pollutant reduction under different urban conditions (wind speeds 1-5 ms^{-1}). The results indicated that the ideal stage of maturity for the vegetation barrier to achieve the most pollutant reduction is from heights of 4-6 m. In this scenario, the vegetation barrier enhances pollutant deposition, has a moderate wake region, and generates a high level of turbulence that promotes downwind pollutant dispersion. It is imperative to account for growth patterns when selecting vegetation as roadside barriers to ensure that it can be maintained through pruning to achieve an ideal barrier height and optimal air pollutant reduction.

Keywords: Air quality, Green infrastructure, Urban green designs, Computational fluid dynamics (CFD), Nature-based solutions

1. Introduction

Exposure to traffic-related air pollution (TRAP) can cause negative health effects, including cardiovascular and respiratory diseases (HEI, 2010; Wilker et al., 2013). Over 45 million people in the U.S. have been estimated to live within 100 m of a major roadway (U.S. Census Bureau, 2009), with minorities and low-income residents more likely to reside at near-road environments (Tian et al., 2013). Millions more people live, work and go to school near large roadways worldwide.

[1] Corresponding author: kz33@cornell.edu

The use of Nature-Based Solutions or green infrastructure (GI) including vegetation to address social and environmental issues is beneficial (Dorst et al., 2019). Roadside vegetation can help alleviate this health burden by reducing TRAP and improving the local air quality in these communities (Baldauf et al., 2008; Al-Dabbous and Kumar, 2014; Gallagher et al., 2015; Baldauf, 2017; Abhijith et al., 2017; Tiwari et al., 2019). However, the physical and ecological attributes of vegetation can strongly influence their capability to reduce local TRAP (Lin et al., 2016; Tong et al., 2016; Deshmukh et al., 2019). Vegetation can primarily reduce pollutants either through deposition, as pollutants settle on the leaves of vegetation, or dispersion, as vegetation alters the airflow around it causing pollutants to dilute (Janhall, 2015). An increased density of vegetation enhances deposition and promotes stronger downwind dispersion (Ghasemian et al., 2017; Deshmukh et al., 2019; Hashad et al., 2020). Vegetation dimensions (width and height), density characteristics leaf area density (LAD) and leaf area index (LAI) influence the capacity to improve air quality downwind of the barrier (Tong et al., 2016; Deshmukh et al., 2019).

For newly planted and existing barriers, the impact of vegetation is dynamic as it will continue to grow over time, leading to spatiotemporal effects linked to its physical and ecological attributes (Bartesaghi-Koc et al., 2020; Corada et al., 2021). While urban planners and local communities can control the barrier's physical characteristics through active maintenance and pruning, no clear best-practice recommendations exist on how to do so while achieving optimal pollutant reduction. It is imperative to understand how vegetation growth over time affects it is capability to mitigate TRAP. Only coniferous vegetation is considered since it has less seasonal variation (maintaining similar leaf area density and therefore pollutant reduction performance throughout the year) and it provides leaf cover from ground level upwards (preventing pollutant to pass unobstructed at ground level). Whereas broadleaf vegetation can lose their leaves in the winter making them ineffective at pollutant reduction, and some broadleaved species have long trunks that might allow pollutants to pass through them unfiltered. Lin et al., 2016 conducted field measurements that showed that vegetation barriers with full foliage reduced ultra-fine particle concentration by 37.7-67.7%, but measurements at the same site during wintertime, when the foliage was reduced, showed no significant change in UFP concentrations. Therefore, broadleaf vegetation that loss their leaves during the winter should not be considered for roadside barriers that are meant to mitigate air pollution year-round. Instead, conifers or evergreen vegetation, which are the focus of this study, should be considered as they are not subject to significant seasonal change (Baldauf 2017). Previous studies of conifers species provide an insight to the impact of vegetation growth on its physical and ecological properties, as its height increases (Pokorney et al. 2008; Malek et al. 2012, Vose et al., 1994). These studies suggest that certain vegetation's LAD can decrease by more than a factor of 5, and its height increase by 7-11 m, over a period of 10-15 years, therefore a vegetation barrier will experience substantial change over time due to vegetation growth.

Stakeholders implementing roadside vegetation barriers to mitigate TRAP must understand the long-term implications of vegetation growth on near-road pollution. This can help urban planners and local communities make informed decisions when designing, planting, and maintaining vegetation barriers. Field measurement studies primarily focus on assessing existing vegetative barriers and how they reduce pollutant concentration. Most of the field measurements usually take place over a period of days or weeks (Lee et al., 2018, Xing and Brimblecombe 2019, Ranasinghe et al., 2019). A few field measurements were conducted over a longer duration (3-5 months) to address the impact of seasonal change on vegetation and TRAP reduction (Lin et al., 2016; Ottosen and Kumar, 2020). In addition, site specific variations relating to the physical and environmental conditions of a vegetation setting require multiple monitoring setups over long time periods. Relying on field measurements alone to assess the impact of vegetation growth on pollutant reduction and develop best-practices in vegetation maintenance is resource intensive and challenging due to varying climate conditions. Computational fluid dynamics (CFD) offers an alternative method to evaluate vegetation barrier designs, under various urban conditions, to understand their impact on near-road air quality (Tong et al., 2016; Santiago et al., 2019; Hashad et al., 2020, Rafael et al. 2018, Li et al., 2022).

To the best of our knowledge, there are no studies that investigated the long-term impact of vegetation growth on pollutant reduction. The objective of this study is to determine how roadside vegetation growth affects the physical mechanisms by which the barrier reduces pollutants through dispersion and deposition. To address that, we first performed a thorough synthesis of existing field studies that examine coniferous vegetation at different ages and characterizes its properties, such as dimensions and density, to understand how vegetation growth impacts its properties, and is presented in Section 2.2. Then, motivated by the key finding from the synthesis we conducted 75 high-fidelity CFD simulations, using the Comprehensive Turbulent Aerosol Dynamics and Gas Chemistry (CTAG) model (Wang et al., 2011; Wang and Zhang, 2012; Wang et al., 2013). The CTAG model has been previously validated against various field measurement studies to ensure that it can properly capture both the aerodynamic and deposition impacts of the vegetation barrier (Steffens et al., 2012; Tong et al., 2016; Hashad et al., 2020) and is discussed in more detail in Section 2.5. The 75 simulations reflect coniferous vegetation barriers in an open-road condition, at various growth stages, with heights ranging from 2-10 m and leaf area index (LAI) varying from 4-11, in order to study their pollutant reduction capabilities. Simulations were undertaken for five different wind speeds (1-5 ms^{-1}) to reflect various urban meteorological conditions. Furthermore, various pollutant particle sizes were modelled to account for traffic exhaust pollution reductions as pollutant deposition on vegetative surfaces, e.g., leaves, is particle size-dependent. Additionally, the downwind spatial decay was analyzed to understand the influence of the barrier on the downwind dispersion of concentrations.

This paper is organized as follows. Sections 2 describes how vegetation growth impacts its properties, the vegetation representation in our simulation, the CTAG model, and the computational domain used in this study. Section 3 discusses the physical mechanisms, by which the various barriers disperse pollutants, and analyze their respective pollutant reduction. Finally, Section 4 is the conclusion.

2. Methods

In this section, we first describe two important vegetation parameters that affect the barrier's pollutant reduction which are the leaf area density (LAD) and the leaf area index (LAI). Then, we present a synthesis of several field measurement studies that document vegetation properties (LAD, LAI, and dimensions) at different ages to understand how vegetation growth affects its characteristics. The results from the synthesis were used to constrain the 75 LES model scenarios highlighted in this study that reflect coniferous vegetation at different ages to understand the influence of vegetation growth on pollutant reduction. The computational approach is then presented, including a description of the domain and boundary conditions, the CTAG model used, how vegetation is represented in the model, and the CTAG model evaluations. Finally, the evaluation criteria used to assess the various vegetation barriers at different growth stages is highlighted. An overview of the Methods section and how it is organized is displayed in Figure 1.

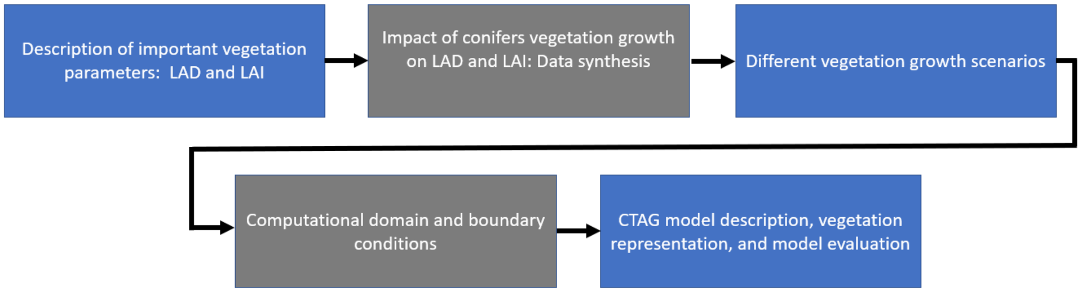

Figure 1: Overview of the methods section

2.1. Vegetation leaf area density (LAD) and leaf area index (LAI)

Vegetation LAD and LAI are two key properties that will influence the pollutant reduction of the vegetation barrier, and it is beneficial to understand how vegetation growth influences them. LAD is a measure of the surface area of leaves per unit volume within the vegetation, units ($\frac{m^2}{m^3}$), and it is an important property affecting vegetation deposition and drag. The LAD profile for coniferous vegetation was considered in this study and can be described by Equation 1 (Lalic and Mihailovic, 2004):

$$LAD(z) = L_m \left(\frac{h - z_m}{h - z}\right)^n \exp\left[n\left(1 - \frac{h - z_m}{h - z}\right)\right],$$

$$where\ n = \begin{cases} 6 & 0 \leq z \leq z_m \\ 0.5 & z_m \leq z \leq h' \end{cases} \qquad (1)$$

L_m is the maximum LAD within the vegetation, z is the height, z_m is the height at which L_m occurs ($z_m = 0.4h$), and h is the vegetation height. This LAD profile has also been used in other CFD modelling studies (Li and Wang, 2018, Xing et al., 2019).

Vegetation leaf area index (LAI) is a unitless metric used to characterize vegetation canopies, defined as the projected area of leaves per ground surface area. If the height and LAI of vegetation is known, the peak LAD, L_m, can be evaluated using Equation 2:

$$LAI = \int_0^h LAD(z)dz \qquad (2)$$

2.2. Impact of vegetation growth on LAI and LAD: Data Synthesis

Understanding how the LAI changes with vegetation growth is important in understanding the mitigation potential of vegetation barriers. We analyzed studies that provided estimates of the LAI for various coniferous vegetation at different ages either through monitoring them over a couple of years as they grow or examining already existing coniferous stands of different ages. Vegetation growth can be described in three growth phases. In the first phase, the vegetation is young and its LAI increases during stand development, as the vegetation crown expands. It reaches its peak LAI during early canopy closure, i.e., when the crowns or canopies of individual trees overlap to form a continuous layer. Fast-growing species can reach their peak LAI in 10-15 years, while slow growing species can reach their peak after 20-40 years (Vertessy et al., 2001; Pokorny and Stojnic, 2012).

Factors such as the local climate, soil type and nutrient availability will affect how fast the vegetation develops. The second phase occurs after this peak, as the LAI decreases to some maximum average LAI that is maintained for years due to canopy closure, competition with other trees, and reduced foliage development (Pokorny´ et al., 2008; Vose et al., 1994). The third phase occurs when the vegetation ages and its LAI eventually starts to decrease as Pokorny and Stojnic (2012) highlighted that the maximum LAI values of spruce stands decreased by 30%, from 12.8 to 8.4, between their peak at 15-20 years to 120 years, due to aging factors (vegetation tissues aging, decreased nutrient supply, and crown abrasion from space competition) (Ryan et al., 1997). In this study, we focused on vegetation in their second development phase, since they reach their peak LAI and achieve canopy closure which is necessary to ensure that it is an effective roadside barrier with no gaps.

Figure 2 and Table 1 highlight the LAI versus vegetation attributes (height of Norway Spruce and age for other conifer species) for vegetation in their second development phase demonstrating that the LAI experiences little change over a substantial age and height range in that stage. The vegetation barriers explored in this study reflect young conifers, Norway Spruce, of heights between 2-10 m and over an 11-year growth period (12-23 years), which is reflected in Figure 2a, and is realistic for roadside barrier applications as highlighted in later sections. In this case, any decrease in the LAI due to aging is not significant. Malek (2010) and Pokorney et al. (2008) showed that the LAI for Norway Spruce increased by a maximum of 0.9-1.6% per year during that growth period (Figure 2a and Table 1). The outcome was similar for trees planted in rows and forest stands, therefore the findings can translate to densely planted vegetation barriers in near-road environments. Due to this small change over a long growth period, a constant LAI of 11 was assumed for the different barriers considered in this study, which aligns with past studies (Pokorny and Stojnic, 2012; Gower and Norman, 1991). Figure 2b and Table 1 also show that other studies found uniform LAI patterns were attained after the peak value for different conifer species such as pine and fir and therefore is a reasonable assumption (Vose et al., 1994; Marshall and Waring, 1986; Zhao et al., 2011; Kim et al., 2017; Barclay et al., 2000; Turner et al., 2000).

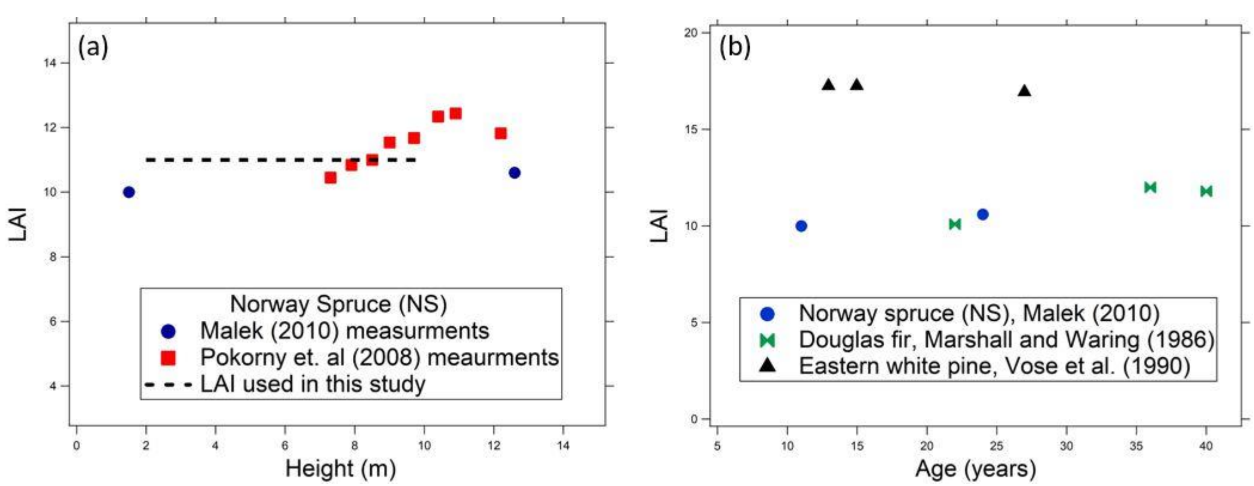

Figure 2: Details of (a) LAI versus vegetation height for Norway Spruce from previous studies compared to LAI value used in this study; and (b) LAI development over time for various coniferous species, which indicates that species maintain a steady LAI after reaching peak LAI.

Table 1: LAI for various conifers species at different ages and heights

Conifers species	Height (m)	Age (years)	LAI	References
Norway spruce	7.3 7.9 8.5 9.0 9.7 10.4 10.9 12.2		10.5 10.8 11.0 11.5 11.7 12.3 12.4 11.8	Pokrony et al. (2008)
Norway spruce	1.5 5 12.6 16.2	11 16 24 29	10.0 10.2 10.6 10.6	Malek (2010)
Douglas-fir		22 36 40	10.1 12.0 11.8	Marshall and Waring (1986)
Eastern white pine		13 15 27	17.2 17.3 16.9	Vose and Swank (1990)
Balsam fir	14.4 13 15	23 29 40	9-11.3 9.5-12.1 8.3-10.9	Derose and Seymour (2010)
Douglas fir		20-80 20-80 20-80	10.6 9.2 12.2	Turner et al. (2000)
Douglas fir		24 33 48	9.6 13.2 11.4	Barclay et al. (2000)
Norway spruce		28	9.88±0.92	Homolova et al. (2007)

Since the LAI for vegetation does not substantially change for the explored height range, this implies that as the height of the vegetation increases, the overall density within the vegetation will decrease as highlighted in Figure 3a. Figure 3b shows the LAD profiles of dense vegetation (LAI = 11) for all heights simulated in this study, which indicates that shorter vegetation is denser compared to taller vegetation. The LAD experiences substantial change, which will influence the vegetation pollutant reduction capabilities as discussed in the results section.

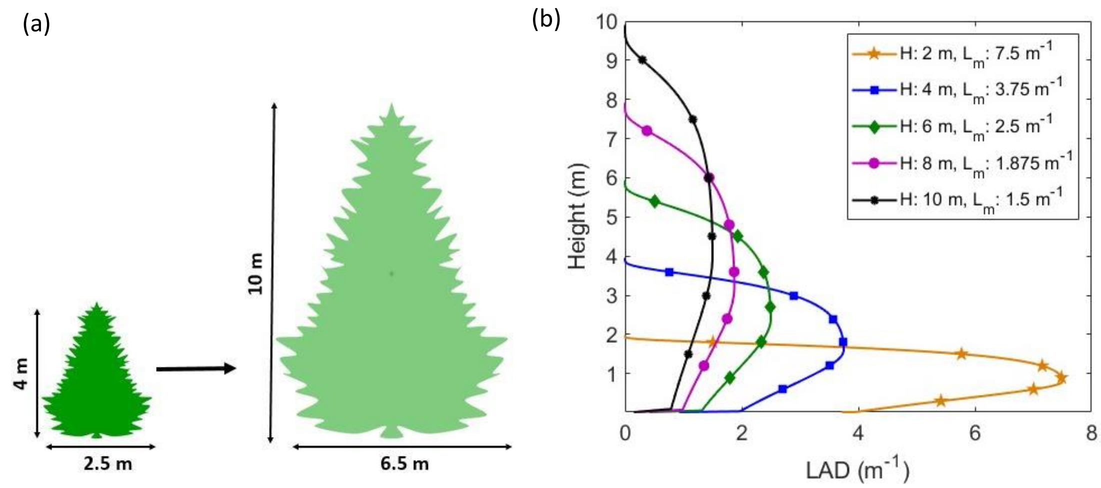

Figure 3: A schematic of (a) the small and large vegetation layouts considered in this study, its LAD decreases as reflected by the faded color representing vegetation density; and (b) the LAD profile for all the dense vegetation (LAI = 11) cases evaluated in this study, where l_m is the maximum LAD that occurs at height z = 0.4h. As the vegetation grows in height its LAD decreases.

2.3. Vegetation dimensions and simulated cases

We investigated vegetation barriers, growing from heights 2 to 10 m, as vegetation shorter than 2 m might not have reached its optimal LAI (still developing) and might allow pollutants emitted by nearby cars and trucks to pass above it, and vegetation taller than 10 m might be challenging to plant and maintain safely for roadside applications. The barrier used in this study consists of two rows of a single type and species of vegetation to reduce any gaps within the barrier. The width (crown length) to height ratio for a single tree was 2/3 reflective of typical coniferous vegetation (Tahvanainen and Forss, 2008; Garber et al., 2009), and has been used in other modelling studies (e.g., Katul et al., 2004). The total barrier width to height ratio was 4/3 since it consisted of two rows of vegetation. Table 2 displays the fifteen different vegetation barrier configurations considered in this study and reflect the barrier at five distinct growing stages (heights 2 – 10 m), and three different densities as represented by the LAI values 4, 7, and 11 to investigate the impact of vegetation growth for various conifers vegetation species with different densities. That ensures that our results not only consider dense conifers like Norway spruce and Douglas fir (LAI = 11), but also other species that might have lower densities (LAI = 4 or 7) (Fassnacht 1997). However, the primary analysis in this study focused on vegetation with an LAI of 11, representing dense conifers, since they are effective roadside barriers compared to less dense vegetation as highlighted later in Section 3.5.

The age and growth rate (0.75 m per year) used in this study were based on the average growth rates of Norway Spruce in those studies (Pokorny et al., 2008; Malek, 2010). The age was rounded to the nearest year, and it is important to note that the age at which vegetation reaches a certain height will depend on several factors such as species, local climate, soil properties, and availability of nutrients (Vose et al., 1994). Therefore, the height and LAI values of the vegetation are better metrics to select vegetation barriers as opposed to age and it can also be applicable to various species that might have different growth rates. Table 2 lists the properties for each barrier configuration, which include the age, height (H), width (W), LAI, and peak LAD (L_m). Each case was tested under five different wind speeds at a height of 10 m (1, 2, 3, 4, and 5 ms^{-1}) to account for various urban conditions, hence 75 total simulations. In addition, 5 simulations were conducted with no barrier at the respective wind speeds to normalize the results.

Table 2: Vegetation barrier properties at various growth stages

Age (Years)	H (m)	W (m)	L_m (m^{-1})		
			LAI=11	LAI=7	LAI=4
12	2	2.5	7.50	4.82	2.75
15	4	5.0	3.75	2.41	1.38
17	6	8.5	2.50	1.60	0.92
20	8	10.5	1.88	1.20	0.69
23	10	13.0	1.50	0.96	0.55

2.4. Computational domain and boundary conditions

Figure 4 displays a schematic of the top and side views of the computational domain for this study. The dimensions of the domain were 60 m along the roadway driving direction, 60 m in the vertical direction, and 250 m in the downwind direction. To represent traffic emissions, two zones of height 3 m and width 14 m each, were used as pollutant sources reflective of a two-way 4 lane traffic bound. A height of 3 m was chosen to account for the initial dispersion of pollutant due to vehicle motion and induced turbulence (Hashad, 2017). This is consistent with other studies that used a traffic zone height of 2.4-3 m (Amorim, 2013; Zheng, 2022). To model vegetation, two zones were created highlighting both rows of vegetation. The vegetation dimensions (height and width) and characteristics (LAD) depend on the simulated case as discussed in the previous sections. The tallest vegetation barrier considered was 10 m, therefore a domain height of 60 m, five times greater than the vegetation height, was selected to ensure no unphysical flow acceleration or blocking effects (Tominaga et al., 2008). The guidelines recommended in Blocken (2015) were followed so a spacing of 5H upstream of the road and a spacing of 15H downwind of the vegetation barrier was used to properly capture the pollutant dispersion of the barrier (Figure 4a). A uniform mesh, with an average cell size of 0.492 m and all hexahedral elements (total of approximately 7.5 million cells), was used as highlighted in Figure S1. A mesh independence study showed that a refined mesh, with a cell sizing of 0.38 m and a total of 14.7 million cells, had little sensitivity with the mesh used, indicating that it captures most of the turbulent kinetic energy (TKE) in the domain (Figure S2).

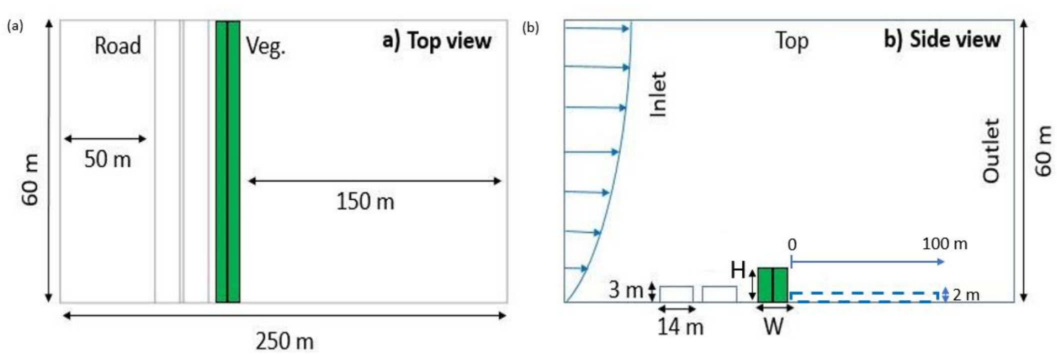

Figure 4: A sketch of the computational domain used in this study a) Top view; b) Side view. The concentrations were averaged from a height of 0-2m starting from behind the vegetation barrier to 100 m downwind of the barrier.

The applied boundary conditions were a neutral atmospheric boundary layer (NABL) velocity profile at the inlet, pressure outflow at the outlet, and symmetry at the top and sides of the domain. To simulate the NABL at the inlet, the velocity described by Equation 3 was used (Richards, 1993):

$$U(z) = \frac{u_*}{k} \ln \left(\frac{z}{z_o}\right) \qquad (3)$$

where U is the velocity, z is the height at which the velocity is evaluated, u_* is the frictional velocity, k is the von Karman constant (=0.4), and z_o is the roughness height (=1 m). In all the simulations, the wind is perpendicular to the barrier to account for the worst-case condition where the community is expected to be exposed to the highest pollutant concentrations. The CTAG model was implemented in this study and is described in the following Section.

2.5. CTAG model description, vegetation representation, and model evaluation

2.5.1 *CTAG model description*

The CTAG model was designed to resolve the flow field including turbulent reacting flows, aerosol dynamics, and gas chemistry in complex urban environments (Wang et al., 2011; Wang and Zhang, 2012; Wang et al., 2013). Large Eddy Simulations were used to resolve the fluid flow and we implemented the dynamic Smagorinsky model to account for the subgrid turbulent viscosity (Germano et al., 1991). The semi-implicit method for pressure linked equation (SIMPLE) algorithm was used to couple the velocity-pressure equations, and a second-order upwind discretization scheme was utilized for all the governing equations.

2.5.2 Vegetation drag and particle deposition in the CTAG model

The CTAG model used is consistent with that of our previous studies on roadside vegetation (Steffens et al., 2012; Tong et al., 2016; Hashad et al., 2020). Since it is computationally expensive to explicitly model the elements of vegetation like branches and leaves, the effects of vegetation on the air flow are spatially averaged and accounted for by adding appropriate sink and source terms to the governing equations (Wilson and Shaw, 1977). To account for vegetation drag, a sink term was included in the momentum equations (Shaw and Schumann, 1992):

$$S_i = -\rho C_d L(z) U u_i, \qquad (3)$$

Where S_i is the sink term, C_d (= 0.3) is the plant drag coefficient, L(z) is the LAD profile, U is the total velocity of the flow, and u_i is the velocity in the direction of interest.

Based on near-road and on-road measurements, nine different particle sizes, ranging from 15 to 253 nm, were included to reflect traffic exhaust emissions (Kittelson et al., 2004; Zhu et al., 2002; Hagler et al., 2012). Since the evaluated particle sizes are small, they were assumed to act as tracers to the flow, hence a one way coupling between the fluid and particles was used. The model did not account for any particle transformation processes, including coagulation, as Steffens et al. (2012) showed that it had a minor impact on pollutant particle size due to their short residence time. A scalar transport equation was used to model pollutant dispersion and deposition. Equation 4 displays the sink term included to the scalar transport equation to account for deposition.

$$S_d(D_p) = \rho V_d(D_p)\widetilde{N_p(D_p)}L(z) \quad (4)$$

Where $\widetilde{N_p(D_p)}$ is the average particle concentration of a particle size D_p, and $V_d(D_p)$ is the deposition velocity adopted from the dry deposition model developed by Zhang et al. (2001). Furthermore, we simulated a tracer gas that does not experience deposition or chemical reactions to capture the effects of barrier on pollutant dispersion. This tracer gas adopted the physical properties of CO but setting the deposition velocity to be zero. The main purpose of using a tracer gas in our simulations was to provide a worst-case scenario, i.e., no reduction by vegetation and we can isolate the effect of dispersion from deposition. The full governing equations for momentum, scalar transport, and deposition velocity are provided in the Section S2 of SI.

2.5.3 CTAG model evaluation

Steffens et al. (2012) assessed the CTAG model using Reynolds-Averaged Navier-Stokes (RANS) simulations against field measurements of both wind speed and particle size distribution, measured behind a near-road vegetative barrier with 6-8 m tall coniferous tree species (Hagler et al., 2012). The field measurements included wind speed data collected at heights 3 and 7 m and 3 m downwind of the barrier, along with ultra-fine particle (UFP) size distributions, ranging from 12.6 to 289 nm. Tong et al. (2016) later evaluated the CTAG model, using LES, against the same field measurements showing better agreement than RANS, since LES better captured the impact of vegetation on the flow. Hashad et al. (2020) also assessed the aerodynamic performance of the CTAG model, using LES against wind speed data collected within and above a maize canopy (Pan et al., 2014) up to twice the height of the canopy. The mean velocity and mean Reynolds stress predicted by the CTAG model reasonably matched those reported in Pan et al. (2014). Section S3 in the SI provides a more detailed description of the field measurements used to evaluate the CTAG model along with a comparison of the CTAG model performance using RANS and LES versus field measurements from our previous studies (Steffens et al. 2012, Tong et al., 2016, Hashad et al., 2020). The evaluation includes particle size distributions, deposition velocities, and fluid flow parameters like mean speed and Reynolds stress.

2.6 Pollutant concentration evaluation criteria

To assess the different vegetation barrier scenarios, the downwind pollutant concentration was averaged over a height of 2 m, covering human breathing height. The spatial decay of concentration was evaluated for 100 m starting behind the barrier (Figures 4b and 5), since pollutant reduction within 100 m is necessary for communities living near roads and exposed to elevated pollutant concentrations. In addition, after 100 m, the pollutant reduction of many vegetation barrier designs is similar. Another metric considered was the average concentration for the 100 m region downwind of the barrier, which can reflect the overall reduction by the barrier. To display the relative reduction in comparison to having no vegetation, the pollutant concentrations have been normalized by the no barrier concentrations at each respective wind speed.

3 Results and Discussion

3.1 Influence of vegetation growth on the barrier's physical dispersion mechanisms

To investigate how vegetation growth affects pollutant dispersion, it is important to first understand how the vegetative barrier alters airflow characteristics, such as velocity and turbulence. Figure 5 displays the velocity, TKE, and normalized concentration contours of the tracer gas for the vegetative barrier at various growth stages. The concentrations were normalized by the corresponding values in the no barrier case. Vegetation induces drag on the flow which slows down the velocity behind the barrier (wake region), but also creates a shear flow around it (low velocity behind the barrier, higher velocity above and around it as shown in Figure 5a). Furthermore, vegetation structures dissipate turbulence (Raupach and Thom, 1981; Finnigan, 2000; Poggi et al., 2004), which creates a region of low turbulence in the wake, followed by a region of high turbulence generated from the shear flow around the barrier as shown in Figure 5b. The concentration plateaus in the wake region due to reduced dispersion in the wake (low velocity and TKE), then it strongly decays due to enhanced TKE, velocity recirculation, and increased velocity after the wake (Figure 5c). Vegetation growth strongly impacts the aerodynamics of the barrier. As it grows taller and less dense, it will produce a longer wake region followed by higher turbulence due to enhanced shear flow (Figures 5a and 5b). Therefore, as the vegetation that forms the barrier matures, the concentration plateau extends for a longer distance before it decays (Figure 5c).

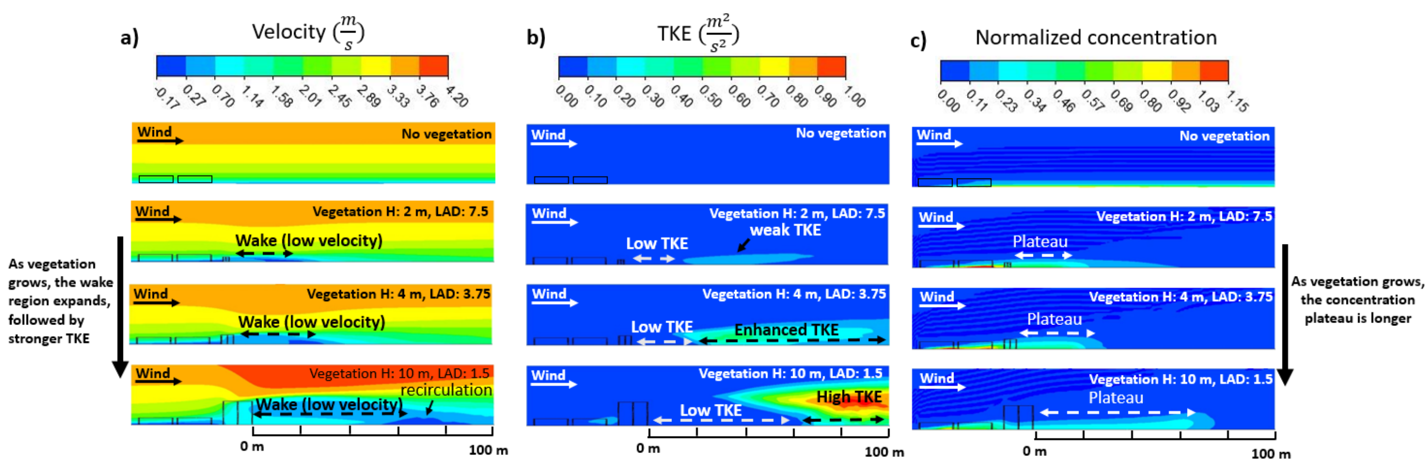

Figure 5: Contours for the no barrier and vegetation barriers at different growth stages with heights 2, 4, and 10 m at a wind speed of 3 ms^{-1} a) Velocity; b) TKE; c) Concentration. As the vegetation grows, the wake region and the concentration plateau extend for a longer distance behind the barrier, and the TKE generated after the wake is enhanced.

3.2 Spatial decay of pollutant concentration at various growth stages

Figure 6 displays the normalized concentration versus distance from the barrier at different ages with heights of 2, 4, 6, 8 and 10 m for particle size 15 nm and wind speed 3 ms^{-1}. The concentrations were normalized by the no barrier concentration at the location immediately behind the barrier (x = 0 m) (Figures 4b and 5). Figure S7 displays the spatial decay for particle size 253 nm. Particles of size 15 nm experience more reduction compared to those of 253 nm, due to enhanced deposition since 15 nm particles have a higher deposition velocity than 253 nm particles. The downwind dispersion for both particles is similar. Figure 6 indicates that the pollutant concentration initially plateaus for a distance roughly corresponding to the wake's length of each barrier.

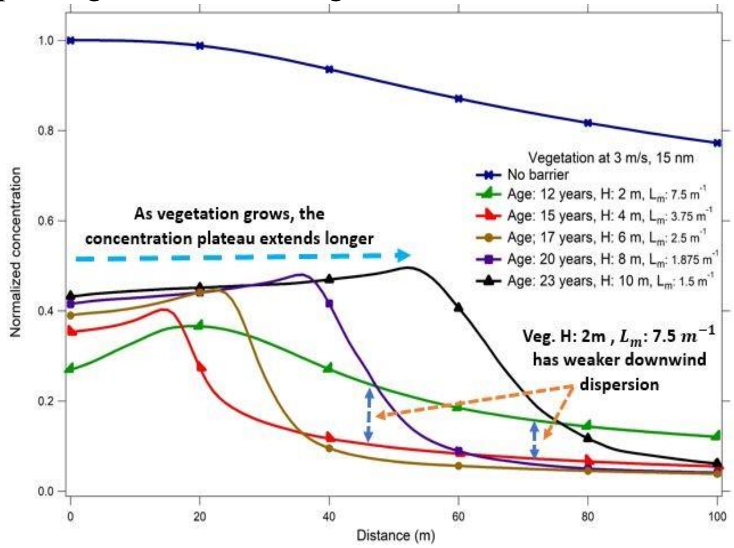

Figure 6: Normalized concentration versus distance from the barrier for the no barrier and vegetation at various ages with heights of 2, 4, 6, 8 and 10 m for particle size 15 nm and wind speed 3 ms^{-1}.

An extended concentration plateau region reduces the barrier's pollutant reduction capability as the pollutant concentrations stagnate. Furthermore, the younger the vegetation, the shorter the plateau region (Figure 6), however, the vegetation needs to mature to a certain height to generate enough TKE to disperse the pollutants downwind of the barrier. Figure 6 shows that the pollutant dispersion, due to the TKE, is weaker for the young vegetation (12 years, H: 2 m, L_m: 7.5 m^{-1}), compared to that of the mature vegetation barriers, as mature (taller) vegetation barriers generate stronger TKE after the wake. Mature vegetation barriers (23 years, H: 10 m, L_m: 1.5 m^{-1}) produced more turbulence after the wake yet had similar downwind pollutant dispersion to that of vegetation with heights of 4, 6, and 8 m (Figure 6). This indicates that the increased turbulence of mature vegetation barriers did not enhance the reduction downwind of the barrier after a certain growth threshold as the concentration becomes well-mixed. Vegetation growth influenced both the length of the plateau region and the strength of the pollutant decay after the plateau.

An ideal barrier will have a short plateau (wake) region followed by a high TKE region to disperse the pollutants. When the vegetation reaches a maturity level, where the height is approximately 4 – 6 m, it generates enough TKE to disperse pollutants downwind, while having a shorter plateau region compared to mature vegetation barriers (heights 8-10 m), resulting in ideal pollutant reduction.

3.3 Influence of vegetation growth on the reduction of particle sizes 15, 253 nm, and tracer gas at extreme wind speeds

Pollutant deposition by the vegetative barrier is particle-size dependent. Particles of size 15 nm experience deposition dominated reduction, while particles of size 253 nm experience dispersion dominated reduction. The velocities evaluated in this study ranged from 1 – 5 ms^{-1}, and the extreme reduction behavior occurred at either wind speeds of 1 or 5 ms^{-1}, depending on the particle size, as discussed later in Section 3.4. An ideal barrier will reduce the concentrations for both particle sizes and wind speeds. Figure 7 shows the normalized average concentration over the 100 m downwind region for particle sizes 15, 253 nm, and tracer gas at wind speeds 1 and 5 ms^{-1} for the vegetation barrier at varying ages and LAI. The tracer gas concentration is slightly higher than particle size 253 nm since that particle size experiences the least deposition.

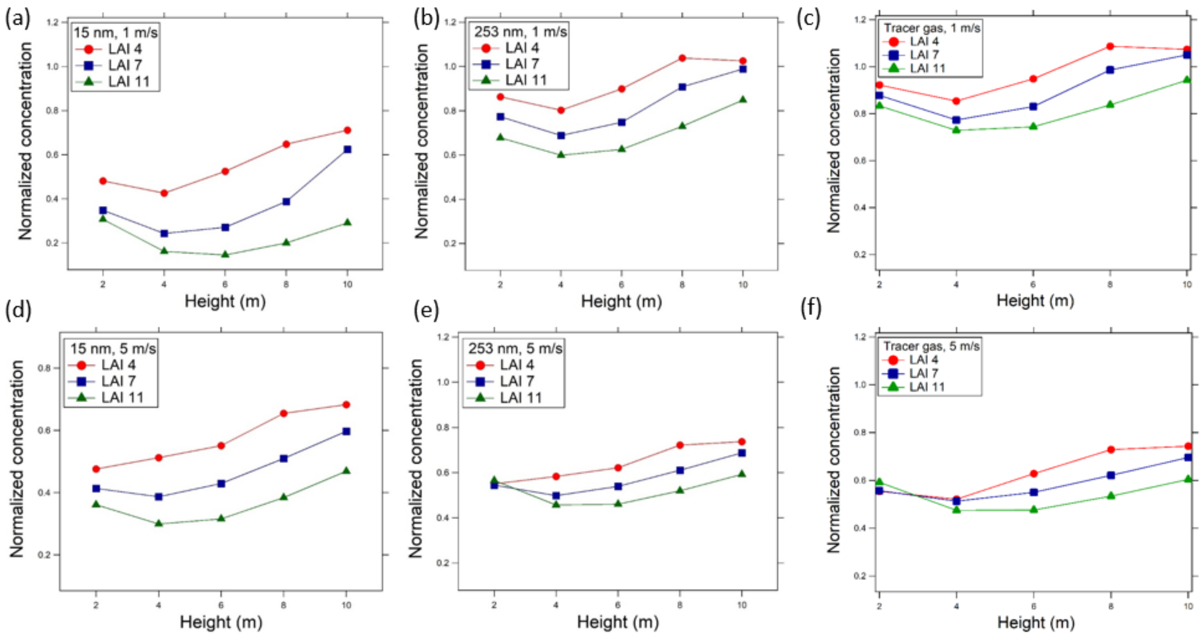

Figure 7: Average concentration over 100 m region downwind of the barrier and height 0 to 2 m, for vegetation barriers at varying ages and LAIs, normalized by the no barrier cases at each wind speed. a) 15 nm, 1 ms^{-1}; b) 253 nm, 1 ms^{-1}; c) Tracer gas, 5 ms^{-1}; d) 15 nm, 5 ms^{-1}; e) 253 nm, 5 ms^{-1}; f) Tracer gas, 5 ms^{-1}.

When the vegetation grows to a height of 4 m, the lowest concentrations were observed as compared to other vegetation barrier heights, when considering different ages, LAI, particle sizes, and wind speeds (Figure 7). This trend was also observed when the concentration was averaged over heights 0 to 3 m and 0 to 4 m (Figures S8 and S9) which ensure that the results were not sensitive to the evaluation criteria chosen, averaging over a height 0 to 2 m. Figures 7a and 7d show that vegetation with height of 4 m had the most reduction for particle size 15 nm which is driven by deposition. Similarly, for particle size 253 nm, where reduction is dominated by the barrier's dispersion, when the barrier matures to a height of 4 m it has the most reduction compared to other barriers. That is due to a shorter wake region followed by enhanced TKE that strongly disperses the pollutants as highlighted in previous sections. While the overall reduction will depend on the particle size, LAI and wind speed, for dense vegetation LAI 11, a 4 m tall barrier can result in twice as much reduction compared to 2 or 10 m tall barriers for wind speed 1 m/s and particle size 15 nm or 17-23% percent reduction for wind speed 5 m/s and particle size 253 nm. It is important to note that for higher LAI values (7-11), which represent denser vegetation, the 6 m barrier resulted in similar reduction compared to the 4 m barrier. Since denser vegetation promote pollutant reduction, a 6 m tall vegetation barrier can also be an ideal vegetation barrier. A 6 m tall barrier could be beneficial especially for highways dominated by trucks, where the emission source is elevated, to ensure that the plume goes through the vegetation. Figure 7 highlights that a barrier, with height of 4-6 m, is optimal when accounting for both deposition and dispersion effects since it results in the most reduction across various LAI values, both particle sizes, and wind speeds.

3.4 Impact of vegetation growth on average concentration (100m region) for various wind speeds and particle sizes

Whether pollutant reduction by the barrier will be dominated by deposition or downwind dispersion (driven by the aerodynamics of the barrier) depends on the wind speed, particle size, and vegetation barrier maturity. To explore these effects, Figure 8 displays average downwind concentrations over the 100 m region for vegetation barriers of different maturity levels (heights 4 and 10 m) for different particle sizes and wind speed conditions. The concentration was normalized by the no barrier concentration at each respective wind speed.

For the vegetation height of 4 m and L_m 3.75 m^{-1} (Figure 8a), particles greater than 70 nm experience more reduction at increasing wind speeds, however, that effect becomes minimal at the highest wind speeds. For particle sizes greater than 70 nm, deposition effects are not dominant, but rather the downwind dispersion of the particles results in concentration reduction, which is enhanced at higher wind speeds due to higher TKE generation by the barrier (Figure S10). On the other hand, for particles less than 70 nm, deposition is more effective and at lower wind speeds, the particles spend more time within the vegetation barrier (increased residence time) which enhances reduction due to deposition. Figure 8b shows that for mature vegetation barriers (Age: 23 years, H: 10 m, L_m: 1.5 m^{-1}), the critical particle size at which the dispersion and deposition effects are dominant occurs at a particle size of 30 nm.

While the physical growth of the vegetation can be captured in terms of height and width, hence particles spend more time within the vegetation, a reduced LAD impacts both the deposition and aerodynamics of the barrier. The study findings indicate that the reduced LAD results in less particle deposition resulting in a shift of particle size. The maturity of the vegetative barrier affects the critical particle size at which the effects of either vegetation deposition or dispersion dominate; thus, a very important parameter accounting for pollutant reductions.

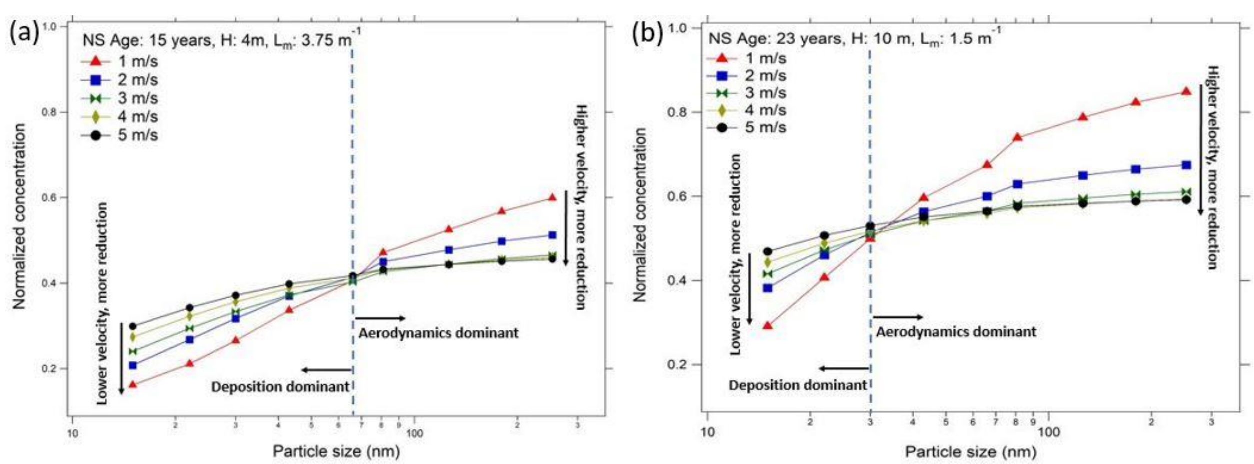

Figure 8: Average concentrations over 100 m region behind the barrier for various particle sizes and wind speeds for vegetation barriers at two different ages. The concentrations were normalized by the no barrier concentrations at the respective wind speeds, a) Vegetation age: 15 years, height: 4 m, L_m 3.75 m^{-1}; b) Vegetation age: 23 years, height: 10 m, L_m: 1.5 m^{-1}.

3.5 Influence of LAI, vegetation species, and LAD profile on pollutant reduction

Figure 7 highlighted an important trend that vegetation with a higher LAI (denser vegetation) will further increase pollutant reduction. Denser vegetation have a shorter wake region and generate higher turbulence downwind of the barrier (Figure 9b), thus promoting pollutant dispersion as highlighted in Figures 9a. While highly porous vegetation does not generate recirculation behind the barrier, denser vegetation produces a ‘detached recirculation’ (Larsen et al., 1999), i.e., occurring further downwind of the barrier after the wake (Figure 9c). The presence of a detached recirculation behind dense vegetation has also been reported in other studies (Cassiani et al., 2008; Detto et al., 2008; Ghasemian et al., 2017). For denser vegetation, not only does the recirculation strength increases, but also it occurs at a distance closer to the barrier because of a shorter wake region (Figure 9c), enhancing early pollutant dispersion.

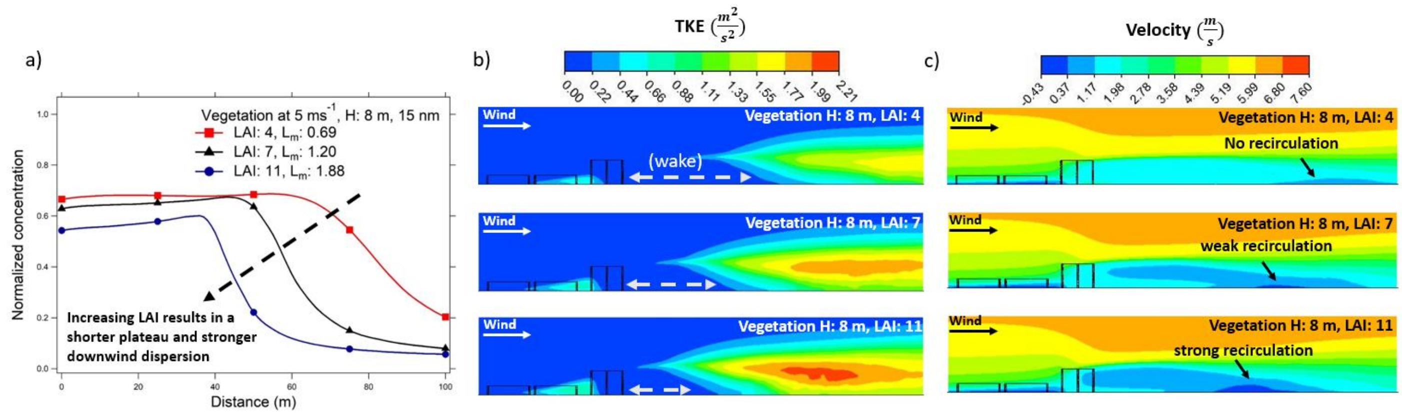

Figure 9: a) Normalized concentrations versus distance from the barrier for vegetation at height 8 m with different LAI reflecting species with varying densities; b) and c) TKE and velocity contours for vegetation at height 8 m and velocity 5 ms^{-1}, vegetation with higher LAI generates higher TKE and have a shorter wake.

High LAD vegetation has an increased surface area for particles to settle on, enhancing deposition compared to vegetation with a lower LAD. In addition, denser vegetation induces more drag on the flow, resulting in lower velocity within the canopy and hence increased residence time for particles, which also promotes deposition. Urban planners will not only benefit from maintaining the barrier at optimal height, but also selecting denser species at the initial planting phase can enhance the overall pollutant reduction of the barrier initially and over time. We also investigated the influence of the LAD profile shape on pollutant reduction. While the LAD profile for conifers vegetation was used in this study, four simulations were conducted with a uniform LAD profile to understand its impact on pollutant reduction. The profile shape had little impact on the downwind dispersion of pollutants; however, there were some differences for deposition dominated scenarios. Overall, the findings in this paper with regards to vegetation growth were not sensitive to this as highlighted in Section S7 of the supporting information (SI).

3.6 Recommendations

This study highlights a few recommendations that urban planners should consider when implementing vegetation barriers to improve air quality at sites experiencing high pollution levels from traffic.

First, urban planners need to consider the vegetation growth rate and maintenance requirements so that they can actively sustain vegetation barriers to an ideal height and achieve optimal post-planting pollutant reduction. According to the American Conifer Society (ACS), conifers species can be split into four size categories that are characterized by the following growth rates per year: miniature (< 2.5 *cm*), dwarf (2.5 – 15 *cm*), intermediate (15 – 30 *cm*), and large (> 30 *cm*). Furthermore, some conifers species are easier to control and prune relative to others. For example, the ACS lists that yews and hemlocks are the easiest to control, and that firs, cedars, spruce and Douglas firs are simple to manage. Additionally, pines require more care when pruning, and junipers, arborvitaes and false cypress are challenging to maintain at a particular size. Factors such as the local climate will influence the vegetation species chosen and how fast it will grow, therefore, stakeholders should select vegetation species that are manageable to prune logistically and temporally given the growth rate of the conifer species they chose for their site.

Second, dense vegetation with high LAI values should be chosen as they are more effective at pollutant reduction due to enhanced deposition and pollutant dispersion downwind of the barrier.

Third, the implemented vegetation barrier height should be around 4 to 6 m to promote pollutant reduction. However, if that is not possible due to factors such as cost or geographical compatibility, at a minimum the vegetation chosen should have matured to their peak LAI which depends on the species. For example, Norway spruce reaches its peak LAI at ages between 10-15 years and at heights between 1.5-2 m. Using younger vegetation, before they reach their peak LAI, is not ideal as they are still developing and hence have lower LAI values, and they might be too short that pollutants can pass above them unobstructed.

Fourth, by identifying the ideal barrier height in the range of 4 to 6 m, urban planners can determine the planting space between trees that will allow for the optimal growth of the barrier.

Finally, in addition to maintaining the barrier at optimal height, other studies have shown that combining vegetation with either low-cost impermeable solid structures (LISS), sound walls, or other vegetation species (low thick bushes) can further enhance pollutant reduction (Tong et al. 2016, Deshmukh et al. 2019, Hashad et al. 2020). This should be implemented, when possible, even if the barrier is maintained at an ideal height. In particular, that could be beneficial when the vegetation is still developing or if it is too tall to further enhance its pollutant reduction capability.

For sites with currently existing vegetation, if the barrier is shorter than the optimal height, the vegetation should be nurtured to reach, and then subsequently maintained, at the recommended height. If it is taller than optimal height, the vegetation should be pruned and maintained at the recommended height if feasible. However, in some sites, pruning to optimal height might be challenging, because either the existing vegetation is too tall, or the species is difficult to prune. In that case, efforts should be made to curb its growth and its pollutant reduction capability can be further promoted by combining it with either solid or vegetation structures.

3.7 Limitations

The pollutant reduction of any vegetation barrier will depend on local conditions, such as atmospheric stability, traffic density and speed, vehicle fleet mix, vehicle induced turbulence, the presence of buildings, roadway configuration and wind direction. While the impact of all these factors were not considered in this study, several key factors likely to dominate the effectiveness of vegetation barriers in reducing local air pollution including wind speed, vegetation dimensions and LAI were explored. Furthermore, the pollutant release height in this study was 3 m which might not fully reflect truck emissions which tend to be at a slightly higher height of approximately 4 m. In addition, all the vegetation barriers considered in this study were implemented close to the highway (5 m distance between the traffic zone and the beginning of the barrier). In addition, the barrier's dimensions, at the different ages considered in this study assumed optimal growth so no gaps existed within the barrier. Ensuring the vegetative barrier is dense with no gaps will rely on the initial plant size, spacing between the planted trees, soil quality to allow for healthy growth, and maintenance and pruning of the barrier after planting. Finally, more field evaluations of the simulation results will enhance the robustness of our recommendations.

4 Conclusion

This paper analyzes how vegetation growth impacts its physical (dimensions) and ecological (density) attributes based on various field measurement studies. Then, we conducted 75 LES simulations to investigate how the growth of roadside vegetation barriers influences TRAP mitigation in near-road environments. Young vegetation barriers (12 years, H: 2 m) provided less downwind pollutant dispersion as a result of reduced turbulence generation compared to mature (taller) vegetation. Mature vegetation (23 years, H: 10 m) created a longer wake region, characterized by low velocity and turbulence, which inhibited pollutant dispersion.

The optimum effectiveness of the barrier to reduce TRAP in a near-road environment was for a vegetation barrier of 4-6 m in height, since it generated sufficient TKE to efficiently disperse pollutants downwind, had a small wake region, and enhanced deposition. The influence of deposition or dispersion as the dominant factor attributed to pollutant reduction using the vegetation barrier varied depending on wind speed (1-5 ms^{-1}), particle size (15 or 253 nm), and the physical (height) and ecological (LAI) attributes of the vegetation. When the barrier matures to 4-6 m, this represents the optimal height to reduce near-road pollutants through both deposition and dispersion, regardless of LAI characteristics. This study demonstrates that as vegetation grows, there is a dynamic and non-linear response in terms of pollutant reduction.

References

Amorim, J. H., Rodrigues, V., Tavares, R., Valente, J., & Borrego, C. (2013). CFD modelling of the aerodynamic effect of trees on urban air pollution dispersion. *Science of the Total Environment*, *461*, 541-551.

Abhijith, K.V., Kumar, P., Gallagher, J., McNabola, A., Baldauf, R., Pilla, F., Broderick, B., Di Sabatino, S., Pulvirenti, B., 2017. Air pollution abatement performances of green infrastructure in open road and built-up street canyon environments – A review. Atmospheric Environment 162, 71–86.

Al-Dabbous, A.N., Kumar, P., 2014. The influence of roadside vegetation barriers on airborne nanoparticles and pedestrians exposure under varying wind conditions. Atmospheric Environment 90, 113–124. URL: http://dx.doi.org/10.1016/j.atmosenv.2014.03.040, doi:10.1016/j.atmosenv.2014.03.040.

Baldauf, R., Thoma, E., Khlystov, A., Isakov, V., Bowker, G., Long, T. and Snow, R., 2008. Impacts of noise barriers on near-road air quality. Atmospheric Environment, 42(32), pp.7502-7507

Baldauf, R., 2017. Roadside vegetation design characteristics that can improve local, near road air quality. Transportation Research Part D: Transport and Environment 52, 354–361. URL: http://dx.doi.org/10.1016/j.trd.2017.03.013, doi:10.1016/j.trd.2017.03.013.

Barclay, H.J., Trofymow, J.A., Leach, R.I., 2000. Assessing bias from boles in calculating leaf area index in immature Douglas-fir with the LI-COR canopy analyzer. Agricultural and Forest Meteorology 100, 255–260. doi:10.1016/S0168-1923(99)00091-X.

Bartesaghi-Koc, C., Osmond, P., Peters, A., 2020.Quantifying the seasonal cooling capacity of 'green infrastructure types' (GITs): An approach to assess and mitigate surface urban heat island in Sydney, Australia. Landscape and Urban Planning 203, 103893.URL:https://doi.org/10.1016/j.landurbplan.2020.103893,doi:10.1016/j.landurbplan.2020.103893.

Blocken, B., 2015. Computational fluid dynamics for urban physics: importance, scales, possibilities, limitations and ten tips and tricks towards accurate and reliable simulations. Build. Environ. 91, 219–245.

Brantley, H.L., Hagler, G.S., J. Deshmukh, P., Baldauf, R.W., 2014. Field assessment of the effects of roadside vegetation on near-road black carbon and particulate matter. Science of the Total Environment 468-469, 120 – 129. URL: http://dx.doi.org/10.1016/j.scitotenv.2013.08.001, doi: 10.1016/j.scitotenv.2013.08.001

Cassiani, M., Katul, G.G., Albertson, J.D., 2008. The effects of canopy leaf area index on air-flow across Forest edges: large-eddy simulation and analytical results. Bound.-Layer Meteorol. 126 (3), 433–460

Corada, K., Woodward, H., Alaraj, H., Collins, C.M., de Nazelle, A., 2021. A systematic review of the leaf traits considered to contribute to removal of airborne particulate matter pollution in urban areas. Environmental Pollution 269, 116104. URL:https://doi.org/10.1016/j.envpol.2020.116104, doi:10.1016/j.envpol.2020.116104.

DeRose, R.J., Seymour, R.S., 2010. Patterns of leaf area index during stand development in even-aged balsam fir - red spruce stands. Canadian Journal of Forest Research 40,629–637. doi:10.1139/X10-018.

Deshmukh, P., Isakov, V., Venkatram, A., Yang, B., Zhang, K.M., Logan, R., Baldauf, R., 2019. The effects of roadside vegetation characteristics on local, near-road air quality. Air Quality, Atmosphere and Health 12, 259–270.

Detto, M., Katul, G.G., Siqueira, M., Juang, J.Y., Stoy, P., 2008. The structure of turbulence near a tall forest edge: the backward-facing step flow analogy revisited. Ecol. Appl. 18 (6), 1420–1435.

Dorst, H., van der Jagt, A., Raven, R., Runhaar, H., 2019. Urban greening through nature-based solutions – Key characteristics of an emerging concept. Sustainable Cities and Society 49, 101620.

Fassnacht, K. S., Gower, S. T., MacKenzie, M. D., Nordheim, E. V., & Lillesand, T. M. (1997). Estimating the leaf area index of north central Wisconsin forests using the Landsat Thematic Mapper. Remote sensing of environment, 61(2), 229-245.

Finnigan, J., 2000. Turbulence in plant canopies. Annual Review of Fluid Mechanics 32, 519–571.

Gallagher, J., Baldauf, R., Fuller, C.H., Kumar, P., Gill, L.W., McNabola, A., 2015. Passive methods for improving air quality in the built environment: A review of porous and solid barriers. Atmospheric Environment 120, 61–70. doi:10.1016/j.atmosenv.2015.08.075.

Garber, S.M., Monserud, R.A., Maguire, D.A., 2009. Modeling crown recession in three conifer species of the northern Rocky Mountains. USDA Forest Service - General Technical Report PNW-GTR 54, 37.

Germano, M., Piomelli, U., Moin, P., Cabot, W.H., 1991.A dynamic subgrid-scale eddy viscosity model. Physics of Fluids A3, 1760-1765.doi:10.1063/1.857955

Ghasemian, M., Amini, S., Princevac, M., 2017. The influence of roadside solid and vegetation barriers on near-road air quality. Atmospheric Environment 170, 108–117. doi:10.1016/j.atmosenv.2017.09.028.

Gower, S., Norman, J.M., 1991. Rapid Estimation of Leaf Area Index in Conifer and BroadLeaf Plantations. Ecological Society of America 72, 1896–1900.

Hagler, G.S.W., Lin, M.Y., Khlystov, A., Baldauf, R.W., Isakov, V., Faircloth, J., Jackson, L.E., 2012. Field investigation of roadside vegetative and structural barrier impact on near-road ultrafine particle concentrations under a variety of wind conditions. Science of the Total Environment 419, 7–15.

Hashad, K., 2017.Comparing different VIT formulations on near-road dispersion of particulate and gaseous pollutants. American Association for Aerosol Research Annual Conference Rayleigh, NC.

Hashad, K., Yang, B., Baldauf, R.W., Deshmukh, P., Isakov, V., Zhang, K.M., 2020. Enhancing the local air quality benefits of roadside green infrastructure using low-cost, impermeable, solid structures (LISS). Science of the Total Environment 717, 137136. URL: https://doi.org/10.1016/j.scitotenv.2020.137136, doi:10.1016/j.scitotenv.2020.137136.

HEI, 2010. Traffic-related air pollution: a critical review of the literature on emissions, exposure, and health effects. Health Effects Institute Special Re, 1–386.

Homolová, L; Malenovský, Zbyněk; Hanuš, Jan; Tomášková, I; Dvořáková, M; Pokorný, R (2007). Com- parison of different ground techniques to map leaf area index of Norway spruce forest canopy. In: ISPRS Working Group VII/1 Workshop ISPMSRS'07: "Physical Measurements and Signatures in Remote Sensing", Davos (CH), 12 March 2007 - 14 March 2007, 499-504.

Janhall, S., 2015. Review on urban vegetation and particle air pollution - Deposition and dispersion. Atmospheric Environment 105, 130–137.

Katul, G.G., Mahrt, L., Poggi, D., Sanz, C., 2004. One- and two-equation models for canopy turbulence. Boundary-Layer Meteorology 113, 81–109. doi:10.1023/B:BOUN.0000037333.48760.e5.

Kim, J., Hwang, T., Schaaf, C.L., Orwig, D.A., Boose, E., Munger, J.W., 2017. Increased water yield due to the hemlock woolly adelgid infestation in New England. Geophysical Research Letters 44, 2327–2335. doi:10.1002/2016GL072327.

Kittelson, D.B., Watts, W.F., Johnson, J.P., 2004. Nanoparticle emissions on Minnesota highways. Atmospheric Environment 38, 9–19. doi:10.1016/j.atmosenv.2003.09.037.

Lalic, B., Mihailovic, D.T., 2004. An Empirical Relation Describing Leaf-Area Density inside the Forest for Environmental Modeling. Journal of Applied Meteorology 43, 641–645. doi:10.1175/1520-0450(2004)043¡0641:AERDLD¿2.0.CO;2.

Larsen, A., Larose, G. L., Livesey, F. M., Robins, A. G., Roberts, P. T., & Speirs, L. J. (1999). Flow and dispersion in the wakes of three-dimensional porous obstacles in a deep, turbulent boundary layer. In *Wind engineering into the 21st century* (1717–1724). Chapter, A A Balkema.

Lee, Eon S., et al. "Field evaluation of vegetation and noise barriers for mitigation of near-freeway air pollution under variable wind conditions." *Atmospheric Environment* 175 (2018): 92-99.

Li, Qi, and Zhi-Hua Wang. "Large-eddy simulation of the impact of urban trees on momentum and heat fluxes." *Agricultural and Forest Meteorology* 255 (2018): 44-56.

Li, Qingman, et al. "Numerical investigations of urban pollutant dispersion and building intake fraction with various 3D building configurations and tree plantings." *International Journal of Environmental Research and Public Health* 19.6 (2022): 3524.

Lin, M.Y., Hagler, G., Baldauf, R., Isakov, V., Lin, H.Y., Khlystov, A., 2016. The effects of vegetation barriers on near-road ultrafine particle number and carbon monoxide concentrations. Science of the Total Environment 553, 372–379. URL: http://dx.doi.org/10.1016/j.scitotenv.2016.02.035, doi:10.1016/j.scitotenv.2016.02.035.

Ma lek, S., 2010. Nutrient fluxes in planted norway spruce stands of different age in southern poland. Water, Air, and Soil Pollution 209, 45–59. doi:10.1007/s11270-009-0180-z.

Marshall, J.D., Waring, R.H., 1986. Comparison of methods of estimating leaf-area index in old-growth Douglas-fir. Ecology 67, 975–979. doi:10.2307/1939820.

Ottosen, T.B., Kumar, P., 2020. The influence of the vegetation cycle on the mitigation of air pollution by a deciduous roadside hedge. Sustainable Cities and Society 53, 101919. URL: https://doi.org/10.1016/j.scs.2019.101919, doi:10.1016/j.scs.2019.101919.

Pan, Y., Chamecki, M., Isard, S.A., 2014. Large-eddy simulation of turbulence and particle dispersion inside the canopy roughness sublayer. Journal of Fluid Mechanics , 499–534doi:10.1017/jfm.2014.379.

Poggi, D., Porporato, A., Ridolfi, L., Albertson, J.D., Katul, G.G., 2004. The effect of vegetation density on canopy sub-layer turbulence. Boundary-Layer Meteorology 111, 565–587.

Pokorny´, R., Stojniˇc, S., 2012. Leaf area index of Norway spruce stands in relation to age and defoliation. Beskydy 5, 173–180. URL: http://beskydy.mendelu.cz/5/2/0173/, doi:10.11118/beskyd201205020173.

Pokorny´, R., Tom´aˇskova´, I., Havra´nkova´, K., 2008. Temporal variation and efficiency of leaf area index in young mountain Norway spruce stand. European Journal of Forest Research 127, 359–367. doi:10.1007/s10342-008-0212-z.

Rafael, S., et al. "Impacts of green infrastructures on aerodynamic flow and air quality in Porto's urban area." *Atmospheric Environment* 190 (2018): 317-330.

Ranasinghe, Dilhara, et al. "Effectiveness of vegetation and sound wall-vegetation combination barriers on pollution dispersion from freeways under early morning conditions." Science of The Total Environment 658 (2019): 1549-1558.

Raupach, M.R., Thom, A.S., 1981. Turbulence in and above Plant Canopies. Annual Review of Fluid Mechanics 13, 97–129.

Richards, P., 1993. Appropriate boundary conditions for computational wind engineering models using the k-ϵ turbulence model. J. Wind Eng. Ind. Aerodyn. 46-47, 145–153. https://doi.org/10.1016/0167-6105(93)90170-s.

Ryan, M.G., Binkley, D., Fownes, J.H., 1997. Age-Related Decline in Forest Productivity: Pattern and Process. volume 27. doi:10.1016/S0065-2504(08)60009-4.

Santiago, J.L., Buccolieri, R., Rivas, E., Calvete-Sogo, H., Sanchez, B., Martilli, A., Alonso, R., Elustondo, D., Santamar´ıa, J.M., Martin, F., 2019. CFD modelling of vegetation barrier effects on the reduction of traffic-related pollutant concentration in an avenue of Pamplona, Spain. Sustainable Cities and Society 48, 101559. URL: https://doi.org/10.1016/j.scs.2019.101559, doi:10.1016/j.scs.2019.101559.

Shaw, R.H.R., Schumann, U., 1992. Large-eddy simulation of turbulent flow above and within a forest. Boundary-Layer Meteorology 61, 47–64. doi:10.1007/BF02033994.

Steffens, J.T., Wang, Y.J., Zhang, K.M., 2012. Exploration of effects of a vegetation barrier on particle size distributions in a near-road environment. Atmospheric Environment 50, 120–128.

Tahvanainen, T., Forss, E., 2008. Individual tree models for the crown biomass distribution of Scots pine, Norway spruce and birch in Finland. Forest Ecology and Management 255, 455–467. doi:10.1016/j.foreco.2007.09.035.

Tian, N., Xue, J., Barzyk, T.M., 2013. Evaluating socioeconomic and racial differences in traffic-related metrics in the United States using a GIS approach. Journal of Exposure Science and Environmental Epidemiology 23, 215–222. doi:10.1038/jes.2012.83.

Tiwari, A., Kumar, P., Baldauf, R., Zhang, K.M., Pilla, F., Di Sabatino, S., Brattich, E., Pulvirenti, B., 2019. Considerations for evaluating green infrastructure impacts in microscale and macroscale air pollution dispersion models. Science of the Total Environment 672, 410–426.

Tominaga, Y., Mochida, A., Yoshie, R., Kataoka, H., Nozu, T., Yoshikawa, M., Shirasawa, T.,2008. AIJ guidelines for practical applications of CFD to pedestrian wind environment around buildings. J. Wind Eng. Ind. Aerodyn. 96 (10−11), 1749–1761.

Tong, Z., Baldauf, R.W., Isakov, V., Deshmukh, P., Max Zhang, K., 2016. Roadside vegetation barrier designs to mitigate near-road air pollution impacts. Science of the Total Environment 541, 920–927. doi:10.1016/j.scitotenv.2015.09.067.

Turner, D.P., Acker, S.A., Means, J.E., Garman, S.L., 2000. Assessing alternative allometric algorithms for estimating leaf area of Douglas-fir trees and stands. Forest Ecology and Management 126, 61–76. doi:10.1016/S0378-1127(99)00083-3.

U.S. Census Bureau, 2009. American Housing Survey for the United States: 2009. URL: https://www.census.gov/content/dam/Census/library/publications/2011/demo/h150-09.pdf.

Vertessy, R.A., Watson, F.G., O'Sullivan, S.K., 2001. Factors determining relations between stand age and catchment water balance in mountain ash forests. Forest Ecology and Management 143, 13–26. doi:10.1016/S0378-1127(00)00501-6.

Vose, J.M., Dougherty, P.M., Long, J.N., Smith, F.W., Gholz, L., Curran, P.J., Curran, J., 1994. Factors Influencing the Amount and Distribution of Leaf Area of Pine Stands. Ecological Bulletins 43, 102–114.

Vose, J.M., Swank, W. T., 1990. Assessing seasonal leaf area dynamics and vertical leaf area distribution in eastern white pine (Pinus strobus L.) with a portable light meter. Tree Physiol 7, 125-134.

Wang, Y. J., DenBleyker, A., McDonald-Buller, E., Allen, D., & Zhang, K. M. (2011). Modeling the chemical evolution of nitrogen oxides near roadways. *Atmospheric Environment*, *45*(1), 43-52.

Wang, Y., Nguyen, M.T., Steffens, J.T., Tong, Z., Wang, Y., Hopke, P.K., Zhang, K.M., 2013. Modeling multi-scale aerosol dynamics and micro-environmental air quality near a large highway intersection using the CTAG model. Science of the Total Environment, 443, 375- 386. URL:http://dx.doi.org/10.1016/j.scitotenv.2012.10.102,doi:10.1016/j.scitotenv.2012.10.102.

Wang, Y.J., Yang, B., Lipsky, E.M., Robinson, A.L., Zhang, K.M., 2013. Analyses of turbulent flow fields and aerosol dynamics of diesel engine exhaust inside two dilution sampling tunnels using the CTAG model. Environmental Science and Technology 47, 889–898.

Wang, Y.J., Zhang, K.M., 2012. Coupled turbulence and aerosol dynamics modeling of vehicle exhaust plumes using the CTAG model. Atmospheric Environment 59, 284-293.

Wilker, E.H., Mostofsky, E., Lue, S.H., Gold, D., Schwartz, J., Wellenius, G.A., Mittleman, M.A., 2013. Residential proximity to high-traffic roadways and poststroke mortality. Journal of Stroke and Cerebrovascular Diseases 22, 366–372. doi:10.1016/j.jstrokecerebrovasdis.2013.03.034.

Wilson, N.R., Shaw, R.H., 1977. A Higher Order Closure Model or Canopy Flow. Journal of Applied Meteorology 16, 1197–1205.

Xing, Yang, and Peter Brimblecombe. "Role of vegetation in deposition and dispersion of air pollution in urban parks." *Atmospheric Environment* 201 (2019): 73-83.

Xing, Yang, et al. "Tree distribution, morphology and modelled air pollution in urban parks of Hong Kong." *Journal of environmental management* 248 (2019): 109304.

Zhang, L., Gong, S., Padro, J., Barrie, L., 2001. A size-segregated particle dry deposition scheme for an atmospheric aerosol module. Atmospheric Environment 35, 549–560.

Zhao, F., Yang, X., Schull, M.A., Roma´n-Colo´n, M.O., Yao, T., Wang, Z., Zhang, Q., Jupp, D.L., Lovell, J.L., Culvenor, D.S., Newnham, G.J., Richardson, A.D., Ni-Meister, W., Schaaf, C.L., Woodcock, C.E., Strahler, A.H., 2011. Measuring effective leaf area index, foliage profile, and stand height in New England forest stands using a full wave form ground-based lidar. Remote Sensing of Environment 115, 2954–2964. URL: http://dx.doi.org/10.1016/j.rse.2010.08.030, doi:10.1016/j.rse.2010.08.030.

Zheng, X., & Yang, J. (2022). Impact of moving traffic on pollutant transport in street canyons under perpendicular winds: A CFD analysis using large-eddy simulations. *Sustainable Cities and Society*, *82*, 103911.

Zhu, Y., Hinds, W.C., Kim, S., Sioutas, C., 2002. Concentration and size distribution of ultrafine particles near a major highway. Journal of the Air and Waste Management Association 52, 1032–1042.